

pubs.acs.org/JPCB Article

Inhibitory Effect of Lanthanides on Native Lipid Flip-Flop

Victoria Cheng and John C. Conboy*



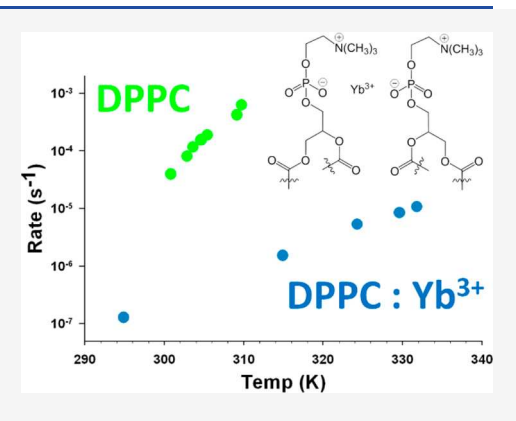
Cite This: J. Phys. Chem. B 2022, 126, 7651-7663



ACCESS

Metrics & More

ABSTRACT: The influence of ytterbium ions (Yb^{3+}) , a commonly used paramagnetic NMR chemical shift reagent, on the physical properties and flipflop kinetics of dipalmitoylphosphatidylcholine (DPPC) planar supported lipid bilayers (PSLBs) was investigated. Langmuir isotherm studies revealed that Yb^{3+} interacts strongly with the phosphate headgroup of DPPC, evidenced by the increases in shear and compression moduli. Using sum-frequency vibrational spectroscopy, changes in the acyl chain ordering and phase transition temperature were also observed, consistent with Yb^{3+} interacting with the phosphate headgroup of DPPC. The changes in the physical properties of the membrane were also observed to be concentration dependent, with more pronounced modification observed at low $(50 \ \mu\text{M}) \ Yb^{3+}$ concentrations compared to 6.5 mM Tb^{3+} , suggesting a cross-linking mechanism between adjacent DPPC lipids. Additionally, the changes in membrane packing and phase transition temperatures in the presence of Tris buffer suggested that a putative $Yb(Tris)^{3+}$ complex forms that



Article Recommendations

coordinates to the PC headgroup. The kinetics of DPPC flip-flop in the gel and liquid crystalline (lc) phases were substantially inhibited in the presence of Yb³+, regardless of the Yb³+ concentration. Analysis of the flip-flop kinetics under the framework of transition state theory revealed that the free energy barrier to flip-flop in both the gel and lc phases was substantial increased over a pure DPPC membrane. In the gel phase, the trend in the free energy barrier appeared to follow the trend in the shear moduli, suggesting that the Yb³+-DPPC headgroup interaction was driving the increase in the activation free energy barrier. In the lc phase, activation free energies of DPPC flip-flop in the presence of 50 μ M or 6.5 mM Yb³+ were found to mirror the free energies of TEMPO-DPPC flip-flop, leading to the conclusion that the strong interaction between Yb³+ and the PC headgroup was essentially manifested as a headgroup charge modification. These studies illustrate that the presence of the lanthanide Yb³+ results in significant modification to the lipid membrane physical properties and, more importantly, results in a pronounced inhibition of native lipid flip-flop.

INTRODUCTION

New studies continue to refine and expose unexpected complexities and dynamics in the ubiquitous lipid bilayer, which is essential to cellular life. Lipid bilayers spatially define a cell and provide a selectively permeable barrier between the cell and its surrounding environment. Cell membranes are composed of various types of phospholipids containing fatty acids with different chain lengths, degrees of unsaturation, and headgroup chemistries with phosphatidylcholine (PC), phosphatidylserine (PS), and phosphatidylethanolamine (PE) being the most common in eukaryotic cells. 1,2 The types of phospholipids are also distributed asymmetrically between the extracellular (outer) and intracellular (inner) leaflets, and this asymmetry is important for cellular function. For example, PS is predominantly found in the inner leaflet, and translocation to the outer leaflet occurs during apoptosis to signal phagocyte recognition and ultimately cell death.3 Lipid compositional asymmetry is maintained through lipid translocation, otherwise known as "flip-flop". Flip-flop has been proposed to be proteinmediated and unidirectional based on the observation that

flippases and floppases can harness ATP to drive unidirectional lipid translocation. $^{4-8}$ However, lipid flip-flop can still occur independently of proteins, though the nature of this process is still under debate. 9,10

Model membranes such as vesicles and planar supported lipid bilayers (PSLBs) have been used to glean insight into the fundamentals of protein-free lipid flip-flop. The myriad of efforts to study lipid translocation all require an asymmetric lipid membrane model to measure the rate of flip-flop. Methods to study lipid translocation in the past have utilized electron paramagnetic resonance (EPR), fluorescence, X-ray scattering, nuclear magnetic resonance (NMR), small-angle neutron scattering (SANS), and neutron reflectivity

Received: June 12, 2022
Revised: September 6, 2022
Published: September 21, 2022





(NR). 7,11,13-17 The first attempt to quantify the rate of flip-flop utilized a TEMPO-labeled 1,2-dipalmitoyl-sn-3-glycerophosphocholine (DPPC) for detection by EPR. 11,18 Vesicles of egg PC and TEMPO-DPPC (TEMPO = (2,2,6,6tetramethylpiperidin-1-yl)oxyl) were incubated with ascorbate, where only TEMPO-DPPC in the outer leaflet was reduced. As lipids exchanged between the inner and outer leaflets, the population of the EPR-active TEMPO-DPPC was replenished in the outer leaflet and subsequently reduced until all the TEMPO-DPPC in the vesicles were removed. From these studies, the rate of flip-flop was measured to be on the order of hours, and hence protein-free lipid flip-flop was assumed to be too slow to be of biological significance. Fluorescence studies of lipid flip-flop used a similar approach employing vesicles containing fluorescently labeled lipids such as NBD-PC (1palmitoyl-2-(6-[7-nitro-2-1,3-benzoxadiazol-4-yl]aminohexanoyl)-sn-glycero-3-phosphocholine). 5,13,19 Fluorescence measurements of lipid flip-flop also obtained rates of translocation on the order of hours, similar to the EPR studies using TEMPO.

Experiments that utilize deuterated lipid species instead of a bulky chemical labels include SANS, NR, and NMR.²⁰⁻²² These studies have been crucial in refining our understanding of the biophysics of the lipid membrane. Studies of lipid flipflop in vesicles by SANS have also reported slow lipid flip-flop rates, but it is difficult to interpret these results without accounting for lipid exchange between vesicles in tandem with lipid flip-flop. 16,23 From these studies, the authors determined half-lives of DMPC flip-flop and intervesicle exchange in the liquid crystalline (lc) phase at 37 °C to be 513 and 151 min, respectively. Similar to SANS, NR provides important measurements of lipid flip-flop in PSLBs. 17 NR studies of asymmetric bilayers composed of perdeuterated 1,2-distearoylsn-3-glycerophosphatidylcholine (DSPCd₈₃) and 1,2-dimyrosityl-sn-glycero-3-phosphatidylcholine (DMPC) found that lipid exchange did not occur on any appreciable time scale at temperatures below the phase transition for DSPC (55 °C) and lipid exchange occurred quickly when both lipids were in the fluid phase. SANS of PSLBs of fluid-phase DMPC and 6 mol % DMPG (1,2-dimystristoyl-sn-glycero-3-phosphatidylglycerol) on 30 nm silica nanoparticles also reported slow flipflop rates, with a reported half-life of flip-flop of ~180 min at 51°C.24

In addition to neutron scattering methods, there are a growing number of studies utilizing NMR on asymmetric vesicles created via methyl- β -cyclodextrin (M β CD) facilitated lipid exchange to study lipid flip-flop in free-floating vesicles in solution. $^{14,25-28}$ For the 1H NMR experiments, M β CD was used to transfer DPPC with perdeuterated headgroups (DPPCd₁₃) to acceptor vesicles made of DPPC with perdeuterated chains (DPPCd₆₂) to yield vesicles with DPPCd₁₃ in the outer leaflet and DPPCd₆₂ in the inner leaflet.¹⁴ In these studies, a paramagnetic shift reagent, Pr³⁺, is required to distinguish the inner and outer leaflets of the membrane. After flip-flop had occurred, an aliquot of the vesicles was exposed to Pr3+ in the solution outside of the vesicle, resulting in distinct NMR chemical shifts of the lipids on the outer leaflet from those in the inner leaflet. Using this approach, the authors found that the rate of DPPC flip-flop occurred on the order of hours to days regardless of lipid phase.14

Although lanthanide paramagnetic shift reagents are extremely useful for ascertaining the location (inside/outside)

of lipid species in a vesicle, it is important to also realize that these reagents also have significant interactions with phoshpolipids. ^{20,29,30} In particular, a study of DMPC vesicles by ¹H NMR and the use of the paramagnetic shift reagent ytterbium (Yb3+) suggested a strong interaction between the Yb³⁺ ion and the phosphocholine headgroup of DMPC, evidenced by significant chemical shifts in the proton resonances upon addition of Yb³⁺. Subsequent MD simulations showed that Yb3+ interacts strongly with the phosphate of DMPC.³¹ ³¹P NMR spectra of 1,2-dioleoyl-sn-glycero-3phosphocholine (DOPC) vesicles in the presence and absence of Pr3+ showed shifts in the 31P signal corresponding to the phosphate group in the headgroup region.²⁹ In addition to the observed chemical shifts, incubating the vesicles with lanthanides also shifted the phase transition temperature, strongly suggesting a change in the physical properties of the bilayer. ¹⁴ It was also suggested that this interaction should have a pronounced effect on lipid flip-flop. ³¹ However, the impact of the lanthanide-lipid interaction on the process of flip-flop has never been investigated.

■ THEORY OF SFVS

Sum-frequency vibrational spectroscopy (SFVS), a complementary method for studying lipid flip-flop, has been shown to be a useful and direct method for probing lipid translocation in model membranes. Similar to SANS and NR, SFVS substitutes a fraction of lipids with deuterated lipids and does not require the use of bulky spin or fluorescent labels. The foundations of SFVS are described in detail elsewhere, and only a brief description follows. FVS is a second-order nonlinear spectroscopy that is forbidden in media with inversion symmetry but allowed at interfaces where the inversion symmetry of the bulk is broken. To obtain a sumfrequency vibrational spectrum, a laser at a fixed visible wavelength is spatially and temporally overlapped with a tunable mid-IR beam at an interface, whereby a beam at the sum of the incident frequencies is generated:

$$\omega_{\rm SF} = \omega_{\rm vis} + \omega_{\rm IR} \tag{1}$$

The SFVS intensity is given by

$$I_{\rm SF} = |\tilde{f}_{\rm SF} f_{\rm vis} f_{\rm IR} \chi^{(2)}|^2 \tag{2}$$

where \tilde{f}_{SF} , f_{vis} , and f_{IR} are the Fresnel coefficients of the electric field intensities of the sum-frequency, visible, and IR beams, respectively. $\chi^{(2)}$ is the second-order nonlinear susceptibility, which is the sum of the resonant $(\chi^{(2)}_R)$ and nonresonant $(\chi^{(2)}_{NR})$ susceptibilities:

$$I_{\rm SF} \propto \left| \left(\chi_{\rm NR}^{(2)} + \sum_{\nu} \frac{A_{\nu}}{\omega_{\nu} - \omega_{\rm IR} - i\Gamma} \right) \right|^2$$
 (3)

where A_{ν} is the product of the IR and Raman transition probabilities and the strength of the transition of the ν vibrational mode, $\omega_{\rm IR}$ is the frequency of the vibrational mode, $\omega_{\rm IR}$ is the frequency of the incident IR beam, and Γ is the intrinsic line width of the vibrational transition. In the specific case of lipid bilayers, we use the methyl symmetric stretch (CH₃ ν_s) intensity from the termini of the fatty acid chains of the lipids as an indicator of bilayer asymmetry. This is achieved by preparing phospholipid bilayers with perdeuterated and protiated leaflets. The intensity of the CH₃ ν_s stretch can be

described in terms of the effective nonlinear susceptibility $\chi_{\text{eff}}^{(2)}$:

$$\chi_{\text{eff}}^{(2)} = \frac{N_{\text{distal}}}{\epsilon_0} \beta_{ijk}^{\text{CH}_3 \nu_s} - \frac{N_{\text{proximal}}}{\epsilon_0} \beta_{ijk}^{\text{CH}_3 \nu_s} + \chi_{\text{NR}}^{(2)}$$
(4)

where $N_{\rm distal}$ and $N_{\rm proximal}$ are the proportion of protiated lipids in the leaflets, proximal or distal, to the solid support, and β_{ijk} is the molecular hyperpolarizability. The measured sum-frequency intensity is related to the measured intensity of the CH₃ ν_s through the following expression:

$$I_{\rm SF} \propto (N_{\rm distal} - N_{\rm proximal})^2$$
 (5)

Initially, the fraction of protiated lipids in each leaflet is asymmetric (for example, $N_{\rm distal}=1$ and $N_{\rm proximal}=0$) in the asprepared bilayer. Interleaflet lipid exchange is described by

$$k_{+}$$

$$N_{\text{distal}} \rightleftharpoons N_{\text{proximal}}$$

$$k_{-}$$
(6)

where k_+ and k_- denote the forward and backward rates of flipflop. As lipids exchange between leaflets overtime, the temporal change in $N_{\rm distal}$ is expressed as

$$\frac{\mathrm{d}N_{\mathrm{distal}}}{\mathrm{d}t} = k_{\perp}N_{\mathrm{distal}} - k_{\perp}N_{\mathrm{proximal}} \tag{7}$$

It has been previously shown that the rate of lipid flip-flop does not depend on the order of deposition (i.e., whether the protiated component is in the distal or proximal leaflet) such that $k_+ = k_- = k$.³² Thus, eq 5 becomes

$$\frac{\mathrm{d}N_{\text{distal}}}{\mathrm{d}t} = -k(2N_{\text{distal}} - 1) \tag{8}$$

and the integrated rate expression is

$$2N_{distal}(t) - 1 = e^{-2kt} (9)$$

where $2N_{\rm distal}-1$ is the population difference of protiated components in each leaflet. From eq 4, the population difference between leaflets is related to the effective nonlinear susceptibility, such that the time-dependent version of eq 4 is described as

$$\chi_{\text{eff}}^{(2)} = |\chi_{\text{R}}| e^{i\varphi_{\text{I}}} e^{-2kt} + |\chi_{\text{NR}}| e^{i\varphi_{\text{I}}}$$
(10)

where $|\chi_R|$ and $|\chi_{NR}|$ are the magnitudes of the complex resonant and nonresonant susceptibilities with phase angles of φ_1 and φ_2 , respectively. When the resonant and nonresonant contributions are in or out of phase, the difference in the phase angles $(\Delta \varphi)$ is taken as 0 or π , respectively. By substituting eq 10 into eq 2, the intensity of the CH₃ ν_s can be expressed as

$$I_{\text{CH}_3\nu_s}(t) = I_{\text{R,max}} e^{-4kt} + 2\sqrt{I_{\text{R}}} \sqrt{I_{\text{NR}}} e^{-2kt} \cos(\Delta \varphi) + I_{\text{NR}} + I_{\text{R,min}}$$
(11)

where $I_{\rm R,max}$ and $I_{\rm R,min}$ are the maximum and minimum intensities of the CH₃ $\nu_{\rm s}$ stretch, respectively. $I_{\rm NR}$ is the nonresonant background intensity, and for the model lipid bilayers on SiO₂, $I_{\rm NR}$ is very small at frequencies where CH vibrational modes in D₂O are absent. Thus, $I_{\rm NR}$ can be removed from eq 11, which simplifies to

$$I_{\text{CH}_3}(t) = I_{\min} + I_{\max} e^{-4kt}$$
 (12)

where $I_{\rm max}$ is the initial signal from the as-prepared asymmetric bilayer and $I_{\rm min}$ accounts for the signal offset of the detection system.

The rate of flip-flop can be related to the free energy of activation (ΔG^{\ddagger}) for the process through the Eyring equation:

$$k = \frac{k_{\rm B}T}{h} \exp \frac{-\Delta G^{\ddagger}}{RT} \tag{13}$$

where $k_{\rm B}$ is the Boltzmann constant, T is temperature, h is Planck's constant, and R is the gas constant. Using SFVS on PSLB models, the impact of membrane packing, headgroup chemistry, chain length, inclusion of transmembrane peptides, and charged peptide interactions on the rate of flip-flop and the energetics of the process have been examined in detail. $^{5,17,33-35}$

In an attempt to elucidate the impact of lanthanides typically used as paramagnetic shift agents in NMR on the rate of lipid translocation, the specific interaction of Yb3+ ions with DPPC lipid membranes was investigated as a model system. The influence of Yb3+ on lipid flip-flop was also correlated to changes in membrane packing by measuring the pressure-area $(\Pi - A)$ isotherms of DPPC in the presence and absence of ${\rm Yb^{3+}}$. In addition, the perturbation of the membrane $T_{\rm m}$ was also measured via SFVS. 36,37 The effect of membrane packing on acyl chain structure was also retrieved from the SFVS spectra. These properties were then correlated to changes in the rate of DPPC flip-flop measured via SFVS in the presence of Yb³⁺. Transition state theory was applied to gain insight into the fundamental energetics of DPPC translocation in the presence and absence of Yb3+. The combinations of these studies have provided strong evidence for the inhibitory effect of Yb3+ on protein-free lipid flip-flop in PSLB model membranes.

MATERIALS AND METHODS

Materials. 1,2-Dipalmitoyl-sn-glycero-3-phosphocholine (DPPC) and 1,2- d_{62} -dipalmitoyl-sn-glycero-3-phosphocholine (DPPCd $_{62}$) were purchased from Avanti Polar Lipids (Alabaster, AL) and used without further purification. Ytterbium chloride hexahydrate (YbCl $_3$ -6H $_2$ O) and deuterium oxide (D $_2$ O) were purchased from Sigma-Aldrich. Tris Base, CHCl $_3$ (HPLC grade), and 30% H $_2$ O $_2$ were purchased from Fisher Scientific. NaOH, concentrated H $_2$ SO $_4$, and 12.1 M HCl were purchased from Macron. All water was obtained from a NanoInfinity water purification system with a minimum resistivity of 18.2 MΩ·cm. The pH of 10 mM Tris buffer from Tris-base was adjusted to a final pH of 7.4 using 2 M HCl.

Π–A Isotherms. Lipid solutions were prepared in 1 mg/mL stock solutions in CHCl₃. Subphases used were pH adjusted water (pH 7), 10 mM Tris, 50 μ M YbCl₃, 6.5 mM YbCl₃, and 6.5 mM YbCl₃ in 10 mM Tris. Twenty-five microliters of 1 mg/mL DPPC was spread over the air/water interface on a KSV minitrough (Helsinki, Finland). The lipid solution was allowed to equilibrate over 10–15 min before compression at a rate of 4 mm/min. A platinum rod with a circumference of 2.553 mm was used instead of a rectangular Wilhelmy plate. All isotherms were collected at room temperature (22.8 ± 0.1 °C).

Shear and Compression Moduli. For the shear and compression moduli experiments, isotherms were collected with a platinum Wilhelmy plate that was oriented either perpendicular or parallel to the direction of compression.

While it would be ideal to have two Wilhelmy plates oriented parallel and perpendicular to the axis of compression, it was previously shown by Cicuta that independent measurements are sufficient to extract information about the moduli. Twenty-five microliters of a 1 mg/mL solution of DPPC was spread at the air/water interface of a KSV minitrough with a subphase of either pH adjusted water, 10 mM Tris, 50 μ M YbCl₃, 6.5 mM YbCl₃, and 6.5 mM YbCl₃ in 10 mM Tris. After allowing the lipid monolayer to equilibrate for 10–15 min, the monolayer was compressed at a rate of 2 mm/min over a distance of 130 mm. Isotherms were smoothed using a 100-point running average. Afterward, the first derivative was taken numerically with a 25-point window.

The compression (K) and shear moduli (G) were calculated via the following equations:

$$K = -\frac{\text{MMA}}{2} \left(\frac{\text{d}\Pi_{\parallel}}{\text{dMMA}} - \frac{\text{d}\Pi_{\perp}}{\text{dMMA}} \right)$$
(14)

$$G = -\frac{\text{MMA}}{2} \left(\frac{d\Pi_{\parallel}}{d\text{MMA}} - \frac{d\Pi_{\perp}}{d\text{MMA}} \right)$$
(15)

where MMA is the mean molecular area (Ų/molecule), Π_{\parallel} is the surface pressure with the Wilhelmy plate oriented parallel to the direction of compression, and Π_{\perp} is the surface pressure with the Wilhelmy plate oriented perpendicular to the direction of compression.

Bilayer Preparation. Bilayers were prepared using the Langmuir-Blodgett/Langmuir-Schaeffer (LB/LS) method, and extensive details about the technique can be found elsewhere.³⁹ Briefly, the fused silica support was submerged in a subphase of water, 50 μ M Yb³⁺, 6.5 mM Yb³⁺, 10 mM Tris, or 6.5 mM Yb3+ in 10 mM Tris. The first (proximal) leaflet contained the deuterated component, DPPCd₆₂. The fused silica prism was first submerged in the appropriate subphase with the long face oriented vertically with respect to the air/ water interface. After 25 µL of DPPC was deposited and allowed to equilibrate for 15 min, the monolayer was compressed to a surface pressure of 30 mN/m at a rate of 4 mm/min. Next, the prism was withdrawn at 3 mm/min via LB deposition. Afterward, the distal leaflet contained protiated DPPC. Similar to DPPCd₆₂, 25 μ L of DPPC was allowed to equilibrate before compression at 4 mm/min to a final surface pressure of 30 mN/m. The prism was then rotated 90° and lowered through the air/water interface with the proximal leaflet to form the LS layer. Measured transfer ratios for the LB and LS layers were 1.1 \pm 0.1. The fully assembled asymmetric bilayer was then transferred and mounted onto a custom Teflon flow cell, which was equipped with ports for solvent exchange and temperature regulation. The bilayer was kept under aqueous conditions during the entirety of the LB/LS procedure and SFVS experiments. The integrity of the PSLBs was periodically tested using fluorescence microscopy as reported previously.⁴⁰ Fluorescence images revealed uniform bilayers within the resolution (~500 nm) of the microscope.

Spectrometer Setup. The 1064 nm output of a Nd:YAG laser (10 Hz, 7 ns pulsed width) was used to pump an OPO/OPA system (LaserVision) to generate a tunable mid-IR source. The 1064 nm laser beam was frequency doubled to generate the 532 nm source. The polarizations of the sumfrequency, 532 nm, and mid-IR beams were s, s, and p, respectively. The 532 nm beam was collimated to 4 mm² with a power of ~7 mJ/pulse. The mid-IR beam was 5 mm² with

 \sim 5 mJ/pulse energy. The generated sum-frequency was detected with a PMT (Hamamatsu Photonics, Hamamatsu, Japan) and the signal averaged with a boxcar integrator (Stanford Research Systems, Sunnyvale, CA). Prior to all spectroscopic data collection, the flow cell was flushed with D₂O or YbCl₃ solutions prepared in D₂O to remove spectral interference from the O–H bands of water. SFVS spectra were collected from 2750 to 3050 cm $^{-1}$ in 2 cm $^{-1}$ steps and integrated for 4 s at each step, and averages of three spectra were taken.

For the kinetics measurements, the temperature of the flow cell was regulated using a circulating water bath (HAAKE, Phoenix II P1 Circulator, Thermo Fisher Scientific). The temperature was monitored inside the flow cell with a type K thermocouple. The intensity of the CH $_3$ ν_s intensity was measured as a function of time while integrating in 3 s intervals.

Phase Transition Temperatures. The intensity of the CH₃ ν_s stretch was measured as a function of temperature in symmetric DPPC bilayers prepared in water, 50 μ M YbCl₃, 6.5 mM YbCl₃, and 6.5 mM YbCl₃ in 10 mM Tris. The temperature was ramped at a rate of 0.4 °C/min from 25 to 65 °C. The intensity of the CH₃ ν_s intensity was recorded by integrating over a 3 s interval. To calculate the $T_{\rm m}$ value, the first derivative of the CH₃ ν_s versus temperature plots were taken, where the inflection point was taken as the $T_{\rm m}$.

RESULTS AND DISCUSSION

 Π -A lsotherms. To explore the impact of Yb³⁺ on DPPC packing in a membrane, Π -A isotherms of DPPC monolayers at the air-water interface were measured. The effect of Yb3+ at millimolar and micromolar concentrations was evaluated to explore the upper and lower bounds of the lanthanide concentrations previously used in NMR studies of lipid bilayers. The influence of Tris buffer was also examined as the ¹H NMR studies by Gonzalez et al. used Tris in addition to Yb3+ in their experiments.20 It has been demonstrated previously that Tris-based buffers may interfere with measurements of vesicles by NMR when lanthanide shift reagents are used.²⁹ For example, Joyce et al. observed differences in Pr³⁺induced peak splitting in ³¹P NMR spectra with and without buffer present. The magnitude of the shift was larger when 3 mM Pr³⁺ was added to 10 mM Tris versus 10 mM HEPES, showing that the identity of the buffer changes the headgroup interaction with Pr3+.29 Thus, in this study the effect of having both Yb3+ and Tris was examined.

The Π -A isotherm of DPPC on a water subphase at pH 7 (Figure 1) showed a typical liquid-expanded (LE) phase for surface pressures below 5 mN/m, a liquid-expanded (LE)/ liquid-condensed (LC) coexistence phase for surface pressures between 6 and 10 mN/m, and a liquid-condensed phase at surface pressures between 10 and 50 mN/m. 22 Above ~50 mN/m the monolayer collapsed. For consistency, all membrane properties are discussed at a surface pressure of 30 mN/m, which is within the range of pressures measured for tension-free lipid vesicles in solution (30-35 mN/m).⁴¹ The measured MMAs at 30 mN/m are presented in Table 1. The baseline mean molecular area (MMA) of DPPC at 30 mN/m in the absence of Yb³⁺ was $45.2 \pm 0.8 \text{ Å}^2$. The MMA of DPPC did not appear to change significantly in the presence of either 50 μ M or 6.5 mM Yb³⁺ compared to a pure water subphase, with measured MMAs of 47.0 \pm 0.3 and 44.9 \pm 0.6 Å², respectively. To account for changes in the MMA due to

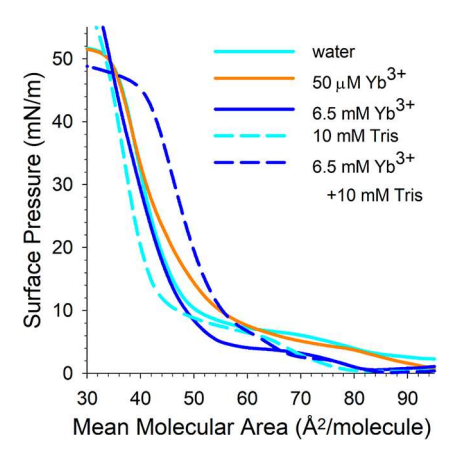


Figure 1. Π –A isotherms of DPPC in water (cyan, solid), 10 mM Tris (cyan, dashed), 50 μ M Yb³⁺ (orange, solid), 6.5 mM Yb³⁺ (blue, solid), and 6.5 mM Yb³⁺ in 10 mM Tris (blue, dashed) represent the average of three replicate isotherms. All isotherms were collected at 22 °C.

Table 1. Mean Molecular Areas of DPPC at 30 mN/m in the Presence of Varying Amounts of Yb^{3+} , Tris, and Yb^{3+} + Tris; Also Tabulated Are the Corresponding MMAs of DPPC at 30 mN/m over a Subphase of NaCl with the Equivalent Ionic Strengths

Subphase	MMA (Ų/molecule) at 30 mN/m	Subphase (NaCl)	MMA (Å ² /molecule) at 30 mN/m
Water	45.2 ± 0.8		
50 μM Yb ³⁺	47.0 ± 0.3	0.6 mM	46.5 ± 0.3
6.5 mM Yb ³⁺	44.9 ± 0.6	78 mM	49.7 ± 0.3
10 mM Tris	42.1 ± 0.5	12 mM	47.2 ± 0.5
6.5 mM Yb ³⁺ + 10 mM Tris	51.3 ± 0.6	90 mM	50.1 ± 0.4

electrostatics, Π –A isotherms of DPPC over subphases composed of NaCl at the same ionic strengths of the YbCl₃ solutions: 0.6, 12, 78, and 90 mM for 50 μ M Yb³⁺, 10 mM Tris, 6.5 mM Yb³⁺, and 6.5 mM Yb³⁺ in 10 mM Tris, respectively (Figure 1), were recorded, and the corresponding MMAs at 30 mN/m are presented in Table 1. The fact that no appreciable shift in the MMA of DPPC was observed, even

when the ionic strength increased 130-fold from 50 µM to 6.5 mM Yb³⁺, points to an interaction between DPPC and Yb³⁺ that cannot be rationalized by electrostatics alone. 42 In a monolayer of phosphatidylcholines, attractive electrostatic interactions between phosphocholine (PC) headgroups contribute to the MMA of DPPC. 42 As the ionic strength of the subphase was increased, the corresponding Debye length decreased, with the upper and lower bounds of the Debye lengths being 12.4 nm (0.6 mM ionic strength) and 1.0 nm (90 mM ionic strength), respectively. With increased ionic strength and a reduced Debye length, the ions in the solution can screen the charges of the PC headgroups, thereby diminishing the attractive interactions between headgroups. A comparison of the MMAs of DPPC in the presence of Yb3+ versus NaCl (Table 1) indicates that the MMA of DPPC are not influenced by changes in ionic strength, but rather a direct interaction between Yb3+ and DPPC.

The observed reduction in the MMA of DPPC in the presence of Yb^{3+} can be attributed to a direct interaction between the Yb^{3+} ions and the phosphate group of DPPC. Yb^{3+} and $PO_4^{\ 3-}$ are known to readily precipitate with solubility products on the order of 10^{-26} M^2 . $^{43-45}$ It was also recently shown that Yb^{3+} will coordinate to DOPC (1,2-dioleoyl-sn-glycero-3-phosphocholine) and DPPC vesicles and interacts with phosphate groups of several PC headgroups at micromolar concentrations. 21 In addition, the NMR study by Joyce et al. also showed a pronounced ^{31}P shift, which would suggest a close association between the lanthanide, Pr^{3+} , and the PO_4 group as the shift agent only works when in close proximity to the nuclei of interest, typically between 2 and 5 Å. 46,47

To evaluate the influence of the Tris buffer on membrane packing in the presence and absence of Yb³+, Π –A isotherms of DPPC in 10 mM Tris and 6.5 mM Yb³+ in 10 mM Tris were collected (Figure 2). The MMA of DPPC in 10 mM Tris decreased to 42.1 \pm 0.5 Ų. However, the monolayer expanded in the presence of both Yb³+ and Tris to 51.3 \pm 0.6 Ų. NaCl subphases with the equivalent ionic strengths as the 10 mM Tris (12 mM NaCl) and 6.5 mM Yb³+ + 10 mM Tris (90 mM NaCl) resulted in an increase in the MMA of DPPC to 47.9 \pm 0.3 and 50.1 \pm 0.4 Ų, respectively (Figure 2 and Table 2). The Π –A isotherm of DPPC condensed in the presence of Tris, which suggests that there is an interaction between DPPC and Tris. It has been previously postulated that the hydroxyl and protonated amine groups from Tris can form hydrogen bonds with the phosphate group in the PC headgroup. ⁴⁸ From the

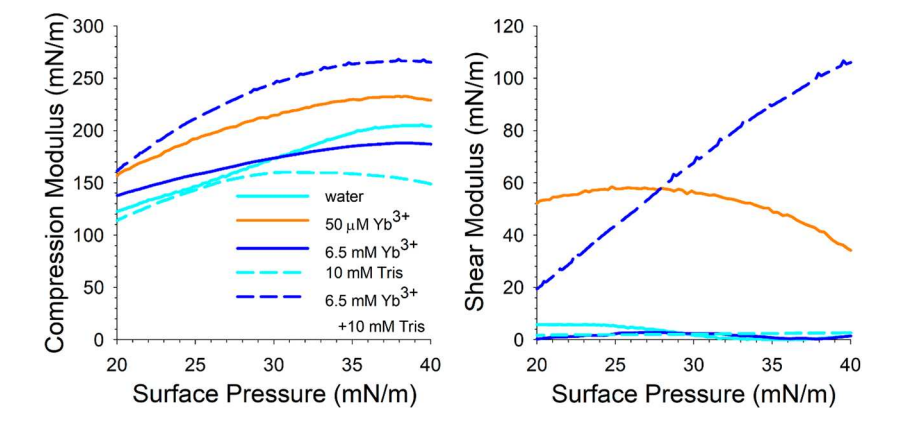


Figure 2. Compression (left) and shear moduli (right) of DPPC with a water (cyan, solid), 10 mM Tris (cyan, dashed), 50 μ M Yb³⁺ (orange, solid), 6.5 mM Yb³⁺ (blue, solid), and 6.5 mM Yb³⁺ + 10 mM Tris (blue, dashed) subphases.

Table 2. Half-Lives of DPPC Flip-Flop at Various Temperatures and in the Presence and Absence of Yb³⁺ and Tris^a

Temp	Half-Life	Temp	Half-Life
(°C)	(min)	(°C)	(min)
50 μM Yb ³⁺		10 mM Tris	
21.7 ± 0.1	45100 ± 200	26.9 ± 0.1	244.1 ± 0.5
28.7 ± 0.1	17600 ± 10	29.8 ± 0.1	65.0 ± 0.4
37.2 ± 0.2	324.7 ± 0.6		
41.8 ± 0.1	3780 ± 20	6.5 mM Yb ³⁺ + 10 mM Tris	
51.1 ± 0.2	1080 ± 10	34.7 ± 0.2	646 ± 7
56.5 ± 0.1	684 ± 8	35.1 ± 0.1	425 ± 3
58.6 ± 0.2	539 ± 10	36.8 ± 0.1	211 ± 2
		37.9 ± 0.1	191 ± 5
6.5 mM Yb ³⁺		38.9 ± 0.2	115 ± 4
20.7 ± 0.2	5500 ± 40	39.2 ± 0.2	101 ± 1
28.6 ± 0.1	966 ± 1	44.6 ± 0.1	1540 ± 20
36.5 ± 0.1	302 ± 1	51.9 ± 0.2	330 ± 1
43.4 ± 0.2	852 ± 10	59.1 ± 0.2	87 ± 2
51.2 ± 0.1	453 ± 4		
55.5 ± 0.1	222 ± 5		

^aThe error in $t_{1/2}$ was propagated from the errors in the fitted rates. The values measured for DPPC flip-flop in Tris are nearly identical to those measured in pure water.

 Π -A isotherms, the presence of both Yb³⁺ and Tris led to an expansion in the membrane, and because 6.5 mM Yb³⁺ and 10 mM Tris separately do not cause the membrane to expand, it seems plausible that Yb3+ and Tris are interacting together to increase the MMA of DPPC. Furthermore, the measured MMA of DPPC in the presence of Yb³⁺ plus Tris exceeds the expected MMA of 50.1 Å² by 1.2 \pm 0.7 Å², which suggests that electrostatics alone cannot be used to rationalize the MMA increase. Tris is known to act as a ligand to lanthanides, evidenced by model complexes such as Eu(Tris)3+ or modified Tris ligands such as La(Bis-Tris)³⁺.49,50 The measured increase in the MMA of DPPC corresponds to an increase in the radius by roughly 1.2 Å, which is also the radius of a Yb(Tris)³⁺ complex, calculated using GaussView 5.0. One hypothesis is that a putative Yb(Tris)3+ complex is coordinated to the phosphate group of DPPC, resulting in the observed increase in the MMA.

If Yb3+ or a Yb(Tris)3+ complex is coordinating with the phosphate of the DPPC headgroup as suggested by the Π -Aisotherms, such an interaction should result in changes in the mechanical properties of the DPPC monolayer. It is worth noting that in lieu of a traditional Wilhelmy plate a Pt rod was used to obtain the Π -A isotherms shown in Figures 1 and 2. The Wilhelmy plate was not used because over the course of the compressions, the Wilhelmy plate was horizontally displaced when positioned orthogonal to the direction of compression. It is well-known that for viscoelastic materials the measured surface pressure as a function of MMA differs when the plate is oriented perpendicular or parallel to the direction of compression (i.e., $\Pi_{\parallel} < \Pi_{\perp}$). When a monolayer undergoes uniaxial compression, the observed response is dependent on both the compression (K) and shear (G) moduli, with the compression modulus representing the response of a material upon a change in area, and the shear modulus describes the response of a material to shear stress.

Shear and Compression Moduli. Using the $\Pi-A$ isotherms, the compression moduli of DPPC at 30 mN/m on a water, 50 μ M Yb³⁺, 6.5 mM Yb³⁺, 10 mM Tris, and 6.5 mM Yb³⁺ + 10 mM Tris subphases were determined to be 187 \pm 8, 218 \pm 5, 179 \pm 8, 167 \pm 9, and 254 \pm 8 mN/m, respectively, from Figure 2. The method used to calculate the compression and shear moduli was taken from Cicuta et al. 51-53 The compression modulus of DPPC on a pure water subphase agrees well with previously reported values. 54,55 The shapes of the compression moduli curves show that the DPPC monolayer is in a single LC phase at a surface pressure of 30 mN/m in the presence of Yb³⁺, Tris, or both Yb³⁺ and Tris. In the presence of 50 μ M Yb³⁺, the compression modulus of DPPC increases by 31 \pm 9 mN/m, while a 6.5 mM Yb³⁺ subphase appears to have no appreciable effect on the compression modulus. By comparison, the presence of 10 mM Tris resulted in a decrease in the compression modulus of the DPPC monolayer to 167 ± 9 mN/m, but the addition of 6.5 mM Yb³⁺ had the opposite effect, increasing K to 254 \pm 8 mN/m. This increase in K of DPPC with a 6.5 mM Yb³⁺ subphase is in contrast to previous studies that have shown a decrease in compressibility in the presence of NaCl, which has been shown by Casillas-Ituarte et al. to interact weakly with the PC headgroup by IR and SFG spectroscopies.⁵⁶ Thus, the increase in K for the DPPC monolayer in the presence of 50 μ M Yb³⁺ and 10 mM Tris and 6.5 mM Yb³⁺ suggests a direct interaction between Yb3+ and DPPC which results in an increase in the rigidity of the membrane.

A more pronounced effect is observed on the shear modulus of DPPC in the presence of Yb³⁺. The calculated shear moduli of DPPC at 30 mN/m with a subphase of water, 50 μ M Yb³⁺, 6.5 mM Yb^{3+} , 10 mM Tris, and $6.5 \text{ mM Yb}^{3+} + 10 \text{ mM Tris}$ subphases were 5 \pm 3, 56 \pm 2, 4 \pm 4, 4 \pm 3, and 67 \pm 8 mN/ m, respectively (Figure 2). The observed maximum shear modulus of DPPC on a water subphase is in agreement with the previously measured shear modulus. 54,55 The slight, nonzero shear modulus of DPPC in the gel state is ascribed to the inability of DPPC molecules to rearrange upon shear stress.⁵⁴ The observed increase in *G* of DPPC in the presence of 50 μ M Yb³⁺ by 65 \pm 4 mN/m suggests more solidlike behavior developing in the monolayer. A possible mechanism for developing a shear modulus in soft materials is the development of a strongly bonded network.³⁸ For example, in poly(vinyl acetate) (PVAc) monolayers at the air/water interface, compression at high surface pressures led to an increase in the shear modulus corresponding to the development of a network of intertwined polymer chains.⁵⁷ The observed changes in the shear moduli of DPPC in the presence of 50 μ M Yb³⁺ and Yb³⁺ + Tris indicate that the monolayer is behaving much like a solid, suggesting a high degree of crosslinking between DPPC lipids.

In light of the changes in the shear moduli of DPPC, we propose that Yb³⁺ coordinates to the phosphate group of PC with different coordination geometries depending on the concentration of Yb³⁺ and presence of Tris. At low concentrations of Yb³⁺, it is possible that one Yb³⁺ ion can coordinate to the phosphate groups of multiple DPPC molecules, leading to a higher shear modulus. Increasing the concentration of Yb³⁺ in solution will favor a lower coordination number of DPPC to Yb³⁺, resulting in a lower degree of cross-linking between DPPC molecules and consequently a lower shear modulus. When both 6.5 mM Yb³⁺ and 10 mM Tris were present in the subphase, the most

significant increase in the shear modulus was observed, increasing the maximum shear modulus from 5 ± 3 to $67 \pm$ 8 mN/m. When Yb³⁺ and Tris are both present, it is possible that the increase in the shear modulus could be due to (1) Tris sequestering free Yb3+ in solution to form a Yb(Tris)3+ complex, which would essentially decrease the effective concentration of Yb³⁺ in solution (i.e., lowering the activity of Yb³⁺), or (2) a putative Yb(Tris)³⁺ complex coordinates multiple phosphate groups from different DPPC molecules, which is supported by the increase in the MMA of DPPC measured for these solutions (see Figure 1 and Table 1). The Π –A isotherms of DPPC on a subphase of 50 μ M and 6.5 mM Yb³⁺ pointed to a headgroup interaction between Yb³⁺ and the phosphate, as has been observed by NMR.20-22 Similarly, the isotherm of DPPC in the presence of Yb3+ plus Tris in the subphase indicate a specific interaction between Yb3+ and DPPC. But the differences in the shear moduli of DPPC in the presence of Yb^{3+} , Tris, and Yb^{3+} + Tris suggest differences in the coordination chemistry between headgroups of DPPC and Yb³⁺. Changes in the properties of the DPPC monolayers are evident in the presence of Yb3+. How these changes are manifest in the chain ordering and phase transition temperature of DPPC bilayers follows.

SFVS Vibrational Spectra. SFVS spectra of asymmetric DPPC bilayers which were prepared with different Yb³⁺ concentrations and in the presence and absence of Tris (Figure 3) provide a molecular level view on the influence of

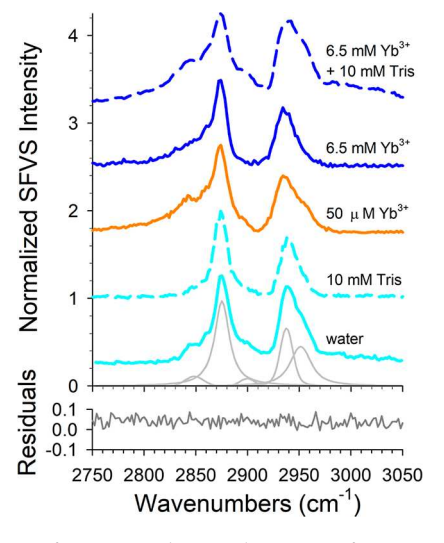


Figure 3. Sum-frequency vibrational spectra of asymmetric DPPC (proximal)/DPPCd₆₂ (distal) bilayers in water (cyan, solid), 10 mM Tris (cyan, dashed), 50 μ M Yb³⁺ (orange, solid), 6.5 mM Yb³⁺ (blue, solid), and 6.5 mM Yb³⁺ + 10 mM Tris (blue, dashed). All spectra were recorded at 21 °C. Spectra are offset for clarity. A representative fit to the spectra in water is shown in gray with the corresponding residuals for the fit.

Yb³⁺ on DPPC chain ordering. The SFVS spectrum of an asymmetric bilayer composed of DPPC in the distal leaflet and DPPCd₆₂ in the proximal leaflet prepared with a water subphase showed the characteristic resonances corresponding to the alkyl chains: symmetric CH₂ stretch (2850 cm⁻¹, CH₂ ν_s), symmetric CH₃ stretch (2875 cm⁻¹, CH₃ ν_s), antisymmetric CH₂ stretch (2900 cm⁻¹, CH₂ ν_a), Fermi resonance of the CH₃ stretch (2936 cm⁻¹, CH₃ FR), and the antisymmetric CH₃ stretch (2950 cm⁻¹, CH₃ ν_a) as shown in Figure 3. ¹⁰

The disorder in the acyl chains can be approximated using the relative integrated peak areas of the CH₂ to CH₃ symmetric stretches $(v_s)^{20}$ Gauche defects result in an increase in the $CH_2 + v_s$ due to a break in the local symmetry of the hydrocarbon backbone. Experimentally, this can be determined from the nonlinear least-squares fit to a Voigt line shape for the vibrational resonances to the spectra and taking the ratio of the CH₂ ν_s and CH₃ ν_s peak areas. From the SFVS spectrum of DPPC in D_2O_2 , the measured $CH_2 \nu_s/CH_3$ $\nu_{\rm s}$ ratio was 0.3 \pm 0.1, suggesting that there exists some degree of gauche conformers within the acyl chains of DPPC. This observation is consistent with previous SFVS experiments and indicative of 1–2 gauche defects per acyl chain as determined from ¹H NMR and IR experiments. ^{39,58–60} In the presence of 10 mM Tris, there was a slight decrease in the CH₂/CH₃ ratio to 0.10, which is consistent with the small decrease in MMA measured in the Π -A isotherms (Figure 1). To rule out spectral contributions of Tris due to the CH₂ groups on the SFVS spectra shown in Figure 3, the spectrum of a symmetric DPPCd₆₂ bilayer prepared in 10 mM Tris was obtained (data not shown). No C-H resonances were observed, which confirms there are no contributions from Tris to the spectra shown in Figure 3 for DPPC. In the presence of 50 μ M Yb³⁺ and 6.5 mM Yb³⁺ the CH₂/CH₃ ratio increased significantly, 1.7 and 1.4, respectively, with more gauche content observed in the presence of 50 μ M Yb³⁺. When both 6.5 mM Yb³⁺ and 10 mM Tris were present, the greatest increase in the relative CH₂ to CH₃ ν_s intensity ratio was observed at 2.5 \pm 0.2. This increase is supported by the 7 Å2 increase in the MMA of DPPC from the Π -A isotherms. In fact, there is a positive correlation between MMA of DPPC and the CH2/CH3 ratios (Figure 5) with R = 0.91 (P = 0.03). This result is not

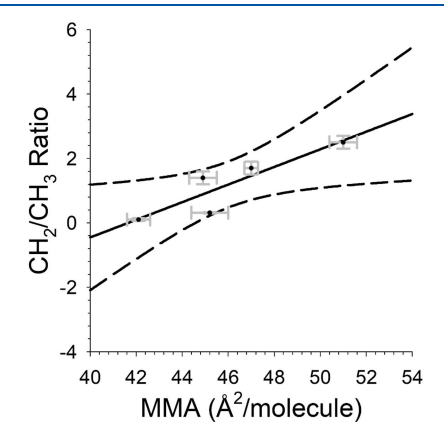


Figure 5. Correlation of the CH₂ $\nu_{\rm s}/{\rm CH_3}$ $\nu_{\rm s}$ peak areas versus the MMA of DPPC. These values were determined using the spectra in Figure 3. The solid black line is the linear regression with the dashed black lines correspond to the 95% confidence interval of the linear fit.

surprising as a larger MMA of DPPC allows the bilayer to accommodate more gauche defects, resulting in an increase in the $\rm CH_2/CH_3$ ratio. 20,39,61

Phase Transition Temperatures. As discussed above, the presence of Yb³⁺ clearly perturbs DPPC packing, compression and shear moduli, and chain order, and these changes should be reflected in the phase transition temperature of the PSLB, as has been reported for solution phase vesicles. We have previously shown that the phase transition temperature of a PSLB can be measured by monitoring the SFVS CH₃ $\nu_{\rm s}$ intensity of the lipid acyl chains as a function of temperature. The present the present the present that the phase transition temperature of the present that the phase transition temperature of the present that the phase transition temperature of the phase transition temperature of the phase transition temperature of the present that the phase transition temperature of the phase transition temperat

As a membrane approaches the $T_{\rm m}$, the phase coexistence of gel and lc phases results in membrane asymmetry, producing an increase in the measured CH₃ ν_s intensity.³⁷ Figure 5 shows the melting curves for DPPC in the present and absence of Tb^{3+} and Tris . The measured T_{m} for DPPC in $\mathrm{D}_{2}\mathrm{O}$ was 41.2 °C, which is in good agreement with the previously determined $T_{\rm m}$ for DPPC in solution phase vesicles.⁶³ In the presence of both 50 µM and 6.5 mM Yb3+, a second phase transition at a higher temperature of 44.7 °C was observed. Marquardt et al. showed via differential scanning calorimetry (DSC) that the $T_{\rm m}$ of DPPC in the presence of Pr³⁺ showed a second distinct phase transition temperature around 44 °C after a first transition at 41 °C, as observed here. They also observed that the magnitude of the shift was not concentration dependent, but rather the intensity of the second phase transition increased with an increase in Pr³⁺ concentration, which is consistent with the SFVS results seen in Figure 6. The

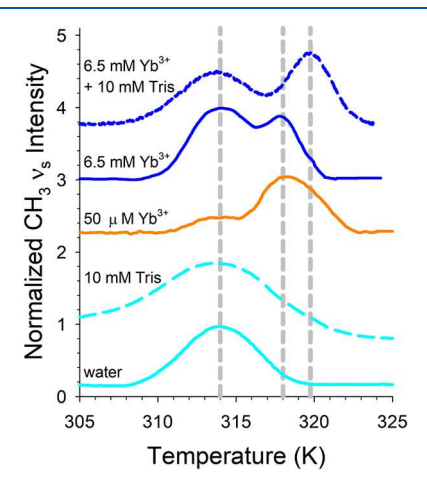


Figure 6. (A) CH₃ ν_s intensity measured as a function of temperature for symmetric DPPC bilayers in D₂O (cyan, solid), 10 mM Tris (cyan, dashed), 50 μ M Yb³⁺ (orange, solid), 6.5 mM Yb³⁺ (blue, solid), and 6.5 mM Yb³⁺ + 10 mM Tris (blue, dashed). The curves have been vertically offset for clarity. The phase transitions were determined by taking the inflection point in the first derivatives of the CH₃ ν_s melting curves. The vertical dashed lines indicating 314 K (41 °C), 317.8 K (44.7 °C), and 320.2 K (47.1 °C).

presence of a second phase transition might be indicative of a second species present in the bilayer due to Yb³⁺ coordinating to the phosphate groups of DPPC, which is suggested by the Π -A, shear moduli, and gauche content in the DPPC membrane discussed previously. The $T_{\rm m}$ describes the amount of thermal energy required for the lipids to transition from the gel to fluid phases. This in part is dictated by the strength of interactions between lipids, and a strong interaction between Yb3+ and DPPC would require more thermal energy to break these interactions in order for the phase transition to occur. The higher $T_{\rm m}$ is attributed to a cross-linked Yb³⁺-DPPC species, while the lower $T_{\rm m}$ should correspond to the monomeric Yb³⁺-DPPC species. In the presence of 50 μ M Yb³⁺, the intensity of the higher $T_{\rm m}$ peak (44.7 °C) suggests that more DPPC is cross-linked via Yb³⁺. However, in the presence of 6.5 mM Yb3+, the relative intensities of the two $T_{\rm m}$'s appear to be about the same, suggesting that fewer DPPC molecules are cross-linked. This observation supports the proposed coordination schemes discussed above, as the

concentration of Yb³⁺ is increased the equilibrium is shifted from the cross-linked species to monomeric coordination.

The role of Tris and Tris plus Yb³⁺ on the phase transition was also investigated. The measured $T_{\rm m}$ of DPPC in 10 mM Tris was 41.5 °C. The absence of a measurable change in the $T_{\rm m}$ of DPPC in the presence of 10 mM Tris is consistent with the small change in MMA, compression, and shear moduli data compared to their values in H2O, presented earlier. However, in the presence of Yb3+ and Tris the second phase transition shifted to a higher temperature of 47.1 °C (vs 44.7 for Yb³⁺ alone), supporting the formation of a Yb(Tris)3+ species that can cross-link DPPC molecules through interactions with Yb3+ and the ability of Tris to chelate multiple Yb3+. It is possible that the presence of Tris could sequester Yb³⁺ in solution, form a putative Yb(Tris)3+ complex, and lower the effective concentration of Yb³⁺. Thus, the phase transition temperatures of DPPC indicate that in the presence of 50 μ M Yb³⁺ there were more cross-linked DPPC molecules that underwent a phase transition at 44.7 °C. If the formation of Yb(Tris)³⁺ complex lowered the effective concentration of Yb3+ in the bulk, the second phase transition observed for DPPC in the presence of Yb³⁺ + Tris should be closer to 44 °C and lower in intensity. Thus, the higher phase transition at 47.1 °C is most likely due to a Yb(Tris)³⁺ complex. The investigations thus far have illustrated the impact of Yb³⁺, Tris, and Yb³⁺ + Tris on the physical properties of the membrane via interactions with the DPPC headgroup. The consequences of these changes on the rate of DPPC flip-flop is examined next.

DPPC Flip-Flop. The rate of DPPC flip-flop was measured as a function of Yb³⁺ concentration and in the presence and absence of Tris to examine the influence of these ions on lipid translocation. Representative plots of the kinetics of DPPC flip-flop are shown in Figure 7. To obtain the rates of DPPC flip-flop, the intensity of the CH₃ ν_s was measured over time and fit to eq 12. From the rates of flip-flop (k), the half-lives $(t_{1/2})$ (Table 2) were calculated via

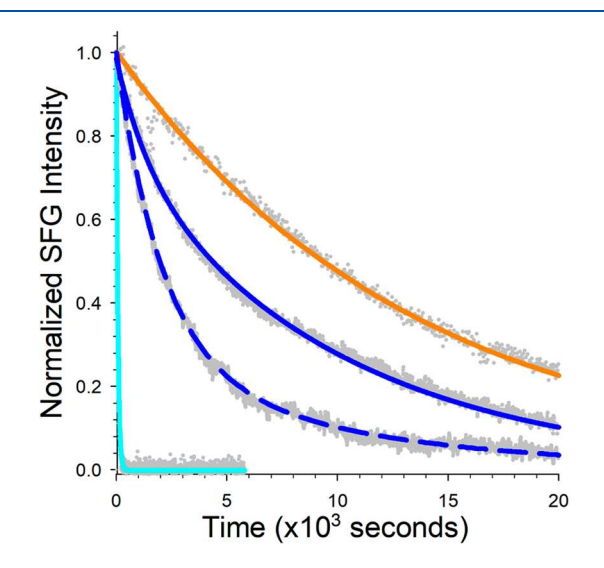


Figure 7. Representative CH₃ ν_s intensity decays as a function of time recorded at roughly 37 °C for DPPC in D₂O (cyan, solid), 50 μ M Yb³⁺ (orange, solid), 6.5 mM Yb³⁺ (blue, solid), and 6.5 mM Yb³⁺ + 10 mM Tris (blue, dashed). The solid lines are the fits to the decays using eq 12.

$$t_{1/2} = \frac{\ln(2)}{2k} \tag{16}$$

Comparisons of the rates as a function of temperature are presented in Figure 8.

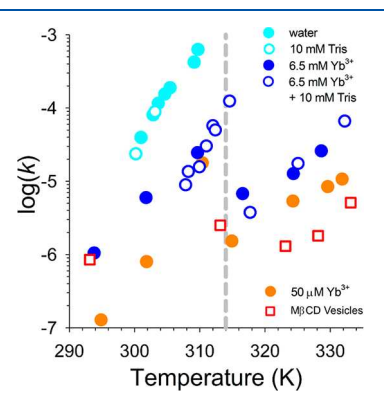


Figure 8. Comparison of the flip-flop rates (seconds) as a function of temperature for PSLBs of DPPC in water (cyan, solid circles), 10 mM Tris (cyan, open circles), 50 μ M Yb³⁺ (orange, solid circles), 6.5 mM Yb³⁺ (blue, solid circles), and 6.5 mM Yb³⁺ + 10 mM Tris (blue, open circles). The reported rates of DPPC flip-flop in solution phase asymmetric vesicles prepared with MβCD and measured by NMR using 66 μ M Pr³⁺ introduced after flip-flop had occurred (red, open squares) from ref 14. The dashed line at 314 K denotes the main $T_{\rm m}$ for DPPC.

The presence of Yb3+ at the concentrations examined strongly inhibited lipid flip-flop of DPPC in the gel phase and lc phases, as depicted in Figure 8. In the gel phase, below 41 °C, the rates of flip-flop in the presence of 50 μ M Yb³⁺ and 6.5 mM Yb³⁺ are about 30 times slower than DPPC in H₂O, and this marked decrease in the rate of flip-flop is supported by the strong Yb3+ interaction with DPPC described above. Either though cross-linking of DPPC lipids or through direct coordination with the phosphate, Yb3+ results in a significant alteration of the headgroup chemistry. It has been previously shown that headgroup modifications can significantly hinder lipid flip-flop. For instance, the $t_{1/2}$ of flip-flop of TEMPO–DPPC in the gel phase at 37 °C was determined by SFVS to be 422 \pm 74 min compared to 9.20 \pm 0.07 min for native DPPC.32 This difference is attributed to the modification of the relatively small choline headgroup by a much larger and chemically different TEMPO group. In addition to size, headgroup charge also plays a role in flip-flop, which has been demonstrated in PSLBs of the negatively charged lipid DSPG (1,2-distearoyl-sn-3-glycerophosphoglyerol) in a DSPC membrane.⁶⁴ The rates of flipflop of both DSPG and DSPC slowed as the DSPG content increased in the PSLB, and this decrease in the rate was attributed to the increasing negative charge in the bilayer. Thus, the decrease in the flip-flop rate of DPPC in the presence of 50 μM Yb³⁺ and 6.5 mM Yb³⁺ observed here are indicative of Yb³⁺-DPPC headgroup interaction, where a net 3+ charge would be imparted to DPPC upon complexation with Yb³⁺. A comparison of the flip-flop rates obtained in the presence of 50 μ M and 6.5 mM Yb³⁺ show that 50 μ M Yb³⁺ has a larger inhibitory impact on the rate of flip-flop (Figure 8), which is supported by the changes in the MMA, compression, and shear moduli reported previously. This observation would

also be consistent with a change in the degree of cross-linking between the phosphate groups of DPPC, as proposed above.

At temperatures near and above the $T_{\rm m}$ of DPPC, there is a marked change in the rate of DPPC flip-flop. The rate of flipflop shows a drastic discontinuity at the phase transition, with a sharp decrease for temperatures above 41 °C when DPPC is the lc phase. Typically, lipid flip-flop in the lc phase of a membrane occurs too quickly to measure by SFVS. 10,32 From Figure 8, the presence of 50 μ M Yb³⁺ and 6.5 mM Yb³⁺ slows down the rate of flip-flop enough to probe the process at temperatures above the main $T_{\rm m}$ of DPPC. More striking is the substantial decrease in the rate of DPPC flip-flop compared to DPPC in water alone. For instance, at 51 °C, the half-lives of DPPC flip-flop in 50 μ M Yb³⁺ and 6.5 mM Yb³⁺ were measured to be 1080 ± 10 and 453 ± 4 min, respectively. In the presence of Yb $^{3+}$ plus Tris, the half-life of flip-flop is ~ 360 min. These are significantly slower than the extrapolated halflife of DPPC flip-flop in D_2O at 51 °C of 0.14 min, which is 2.6 \times 10³-7.7 \times 10³ times faster than when Yb³⁺ and Tris or 50 μ M Yb³⁺ are present. Clearly, the interaction between Yb³⁺ and DPPC has a very large influence on the rate of DPPC flip-flop in the lc phase compared to the gel state. This is also consistent with NMR and fluorescence microscopy studies which have shown that lanthanides interact strongly with phospholipids in the lc phase. 29,65-67

The effect of Tris buffer did not have any apparent influence on the rate of DPPC flip-flop, evidenced by the similar $t_{1/2}$ in 10 mM Tris and D₂O at 29 °C (Table 2). However, Tris in the presence of 6.5 mM Yb³⁺ significantly changes DPPC flip-flop, consistent with the observed changes in membrane structure discussed above. At 37 °C, the $t_{1/2}$ of DPPC flip-flop was 235 \pm 2 min, which is still significantly slower than DPPC in water but also faster than Yb³⁺ alone. The slower rate of flip-flop would suggest that the network of bonds between Yb(Tris)³⁺ is similar to those found in the DPPC bilayer in the presence of 50 μ M Yb³⁺. Thus, the introduction of Tris, which occupies coordination sites on Yb³⁺, could promote cross-linking between other Yb³⁺ and adjacent DPPC lipids. The increase in coordination between Yb³⁺ plus Tris could explain the relatively faster rate of flip-flop compared to 6.5 mM Yb³⁺ alone.

The measured rates of DPPC flip-flop illustrate the consequences of Yb3+-DPPC interactions. The presence of 50 μ M Yb³⁺ and 6.5 mM Yb³⁺ clearly slowed the rate of flipflop with 50 μ M Yb³⁺ having a more significant impact on the rate than 6.5 mM Yb3+. These changes are consistent with the proposed coordination schemes of Yb3+ to the DPPC headgroup suggesting a cross-linked network of DPPC lipids. Tris buffer did not appear to change the kinetics of DPPC flipflop, despite slight changes in the MMA of DPPC. The most striking observation is that the strong interaction between Yb³⁺ and DPPC allowed the rate of flip-flop to be obtained at temperatures above the $T_{\rm m}$. The measured decrease is most pronounced in the presence of 50 μ M Yb³⁺, with a flip-flop rate 7.7×10^3 times slower than DPPC in D₂O at 51 °C. A comparison of the measured flip-flop rates in the presence and absence of Yb3+ demonstrates that lanthanides dramatically decreases the rates of flip-flop as measured by SFVS. The rates suggest that the headgroup interaction between lanthanides and the phosphate group causes the observed inhibition in flipflop. Knowing the rates in the gel and lc regimes, transition state theory was applied to gain insight into the effect of Yb3+ and Yb(Tris)³⁺ on the underlying energetics of DPPC flip-flop.

Transition State Thermodynamics. The free energies of activation (ΔG^{\ddagger}) for DPPC flip-flop in the presence of Yb³⁺ were calculated from the flip-flop rates (Figure 8 and Table 2) using the Eyring equation (13). The calculated ΔG^{\ddagger} are plotted as a function of temperature (Figure 9). The transition

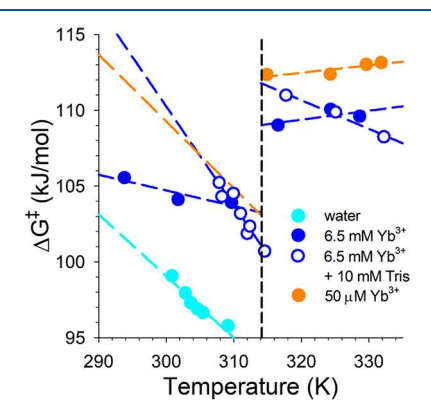


Figure 9. Transition state energies as a function of temperature for DPPC flip-flop in D_2O (cyan, solid circles), $50~\mu M$ Yb³⁺ (orange, solid circles), 6.5~mM Yb³⁺ (blue, solid circles), and 6.5~mM Yb³⁺ + 10~mM Tris (blue, open circles) with the corresponding fits using eq 17 noted as the dashed lines. The vertical dashed lined at 314 K denotes the main T_m for DPPC. Data for DPPC in D_2O are taken from ref 32 and are included for comparison.

state enthalpies (ΔH^{\ddagger}) and entropies (ΔS^{\ddagger}) for each of the Yb³⁺ concentrations studied were determined using the Gibbs equation (17).

$$\Delta G^{\ddagger} = \Delta H^{\ddagger} - T \Delta S^{\ddagger} \tag{17}$$

It was found that there was strong entropy-enthalpy compensation (Figure 10), so the following discussion does

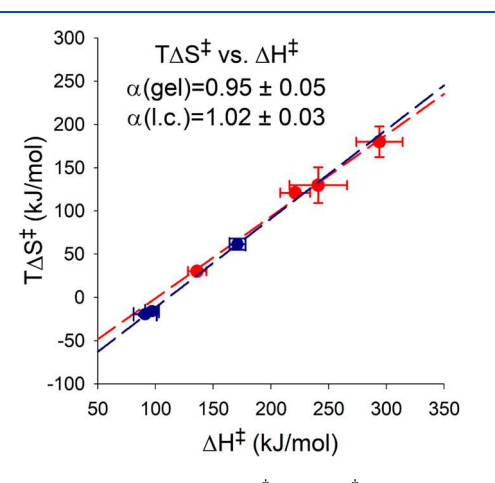


Figure 10. Correlation between $T\Delta S^{\ddagger}$ and ΔH^{\ddagger} for DPPC flip-flop in the gel (blue) and lc (red) states with the slopes (α) shown for comparison. The temperature was set to 295 K for the determination of $T\Delta S^{\ddagger}$.

not weight too heavily the individual contributions from either enthalpy or entropy.⁶⁸ To account for the discontinuity in the flip-flop rates of DPPC in the gel and lc states, these regions where treated independently for the two temperature regimes, and the following discussion proceeds with an initial examination of activation thermodynamics in the gel state followed by the lc state.

Gel State. The activation free energy of DPPC flip-flop in the presence of Yb³⁺ increased at all temperatures examined below 314 K. For instance, at 298 K, the free energy of DPPC flip-flop was previously determined to be 99 kJ/mol.³² The presence of 6.5 mM Yb3+ increased the free energy barrier to about 104 kJ/mol, and the presence of 50 μ M Yb³⁺ and Yb³⁺ + Tris further increased the activation free energy barrier to 110 and 112 kJ/mol, respectively, at 298 K. The activation free energy is shaped by factors such as intermolecular interactions (e.g., headgroup interactions, van der Waals interactions between acyl chains) and water reorganization at the lipidwater interface. 10 The increases in the activation free energy are correlated to changes in the shear moduli of membrane. This suggests that coordination of DPPC by Yb3+ or Yb3+ + Tris might be impacting the observed changes in the activation thermodynamics. At 298 K, the DPPC monolayer in the presence of Yb³⁺ + Tris had the largest shear modulus, and the ΔG^{\ddagger} of flip-flop was found to be the largest, followed by the shear modulus and ΔG^{\ddagger} of DPPC flip-flop in the presence of 50 μ M Yb³⁺. In the presence of 6.5 mM Yb³⁺, the shear modulus of DPPC did not appear to change appreciably in comparison to the shear modulus of DPPC over a pure water subphase, though the $T_{\rm m}$ shift strongly pointed to a headgroup interaction between Yb³⁺ and the phosphate of the headgroup. More energy would be required to break this headgroup interaction to facilitate DPPC flip-flop.

Liquid-Crystalline State. At temperatures above the main $T_{\rm m}$, the activation free energy of DPPC was generally higher in the fluid phase than the gel phase. This suggests that the DPPC headgroup interaction with Yb3+ is stronger in the lc state compared to the gel phase. Interestingly, the ΔG^{\ddagger} of DPPC flip-flop increases with temperature in the presence of 50 μM Yb³⁺ and 6.5 mM Yb³⁺. In a previous study of TEMPO-DPPC flip-flop, the activation free energies also followed this trend: the TEMPO headgroup modification strongly inhibited flipflop, and the activation free energy increased with increasing temperature. This added energetic penalty was ascribed to a negative entropy related to the solvation/desolvation of TEMPO headgroup.³² In the current studies of Yb³⁺ and DPPC, the transition state free energies strongly suggest that the interaction between Yb3+ and the phosphate group of the lipids is akin to a headgroup modification. The bound Yb³⁺ not only increases the size of the headgroup but also imparts a + 3 charge. Similar to the presence of 50 μ M Yb³⁺ and 6.5 mM Yb^{3+} , the presence of Yb^{3+} + Tris increases the activation free energy barrier in the fluid phase. In contrast to the presence of 50 μ M Yb³⁺ and 6.5 mM Yb³⁺, the activation free energy barrier of DPPC flip-flop in the presence of Yb3+ + Tris decreased with increasing temperature, which points to a different type of interaction between the phosphate headgroup and Yb³⁺ + Tris. It is worth noting that the presence of Yb³⁺ and Yb3+ + Tris allowed for the first measurements of DPPC flip-flop in the fluid phase by SFVS. These studies demonstrate that the presence of Yb³⁺ reduces the rate of flip-flop, which is consistent with previous measurements, through an interaction with the phosphate headgroup of PC. More importantly, these results highlight the fact that Yb3+ and lanthanide shift reagents, in general, have profound effects on the rate of lipid translocation. Our results also demonstrate that the presence of both Yb3+ + Tris resulted in different physical properties of DPPC monolayers and flip-flop kinetics, which we attribute to a putative Yb(Tris)³⁺ complex. The Yb(Tris)³⁺ complex could interact with the phosphate headgroup of DPPC and cross-link DPPC molecules, as was the case with 50 μ M Yb³⁺ present, and these headgroup interactions were found to increase the free energy barrier to flip-flop, thereby decreasing the rate of flip-flop.

CONCLUSIONS

The studies on the impact of Yb3+ on membrane properties and DPPC flip-flop presented herein demonstrate that at concentrations used in typical ¹H NMR experiments the presence of Yb $^{3+}$ and Yb $^{3+}$ + Tris have significant implications for measuring lipid translocation. In terms of membrane packing, the changes in MMA were small in the presence in 50 μ M Yb³⁺ and statistically insignificant in the presence of 6.5 mM Yb³⁺, when Yb³⁺ + Tris were present, but the MMA increased significantly, and the change in MMA corresponded to the presence of a Yb(Tris)3+ complex, as ionic strength alone could not account for the magnitude of the increase. Mechanical properties of the DPPC membrane in the presence of Yb3+ was characterized by the shear moduli. The shear moduli of DPPC in the presence of 50 μ M Yb³⁺ and 6.5 mM Yb³⁺ showed that Yb³⁺ can coordinate with the phosphate headgroups of several DPPC molecules. The presence of an interaction between Yb3+ and the phosphate headgroup was further supported by the presence of a second phase transition temperature, measured by SFVS. Similarly, an interaction between Yb(Tris)3+ and DPPC was supported by changes in the shear moduli and phase transition temperature. The fact that the second phase transition in the presence of Yb(Tris)³⁺ was at a higher temperature suggests that a Yb(Tris)³⁺ complex was responsible and not free Yb3+. The consequences of these changes were manifested in the flip-flop rates which were significantly inhibited, which also supports the proposed models of Yb3+ or Yb(Tris)3+ coordination to the phosphate headgroup of DPPC. Interestingly, the rate of DPPC flip-flop was slow enough to measure in the lc phase when Yb3+ or Yb(Tris)3+ was present. While the rate of flip-flop was inhibited with either Yb3+ or Yb(Tris)3+, the underlying energetics of flip-flop were significantly different in the gel versus lc phases. The changes in the transition state energetics of DPPC flip-flop in the presence of 50 μ M and 6.5 mM Yb³⁺ mirrored the transition state parameters of flip-flop of TEMPO-DPPC, which show a decrease in both ΔH^{\ddagger} and ΔS^{\ddagger} . These changes strongly support an interaction between Yb³⁺ and the phosphate headgroup of DPPC that is similar to the headgroup modification in TEMPO-DPPC. The combined Langmuir monolayer studies and SFVS measurements demonstrate that interactions between Yb3+ and DPPC have a significant inhibitory effect on lipid translocation.

AUTHOR INFORMATION

Corresponding Author

John C. Conboy – Department of Chemistry, University of Utah, Salt Lake City, Utah 84112, United States; orcid.org/0000-0003-0023-642X;

Email: Victoria.Cheng@law.utah.edu

Author

Victoria Cheng – Department of Chemistry, University of Utah, Salt Lake City, Utah 84112, United States

Complete contact information is available at: https://pubs.acs.org/10.1021/acs.jpcb.2c04039

Notes

The authors declare no competing financial interest.

ACKNOWLEDGMENTS

This research was supported by funds from the National Science Foundation (NSF 1953975).

REFERENCES

- (1) Van Meer, G.; Voelker, D. R.; Feigenson, G. W. Membrane Lipids: Where They Are and How They Behave. *Nat. Rev. Mol. Cell Biol.* **2008**, 9 (2), 112–124.
- (2) Lehninger, A. L.; Nelson, D. L.; Cox, M. M. Principles of Biochemistry; W.H. Freeman and Company: New York, 2008.
- (3) Ikeda, M.; Kihara, A.; Igarashi, Y. Lipid Asymmetry of the Eukaryotic Plasma Membrane: Functions and Related Enzymes. *Biol. Pharm. Bull.* **2006**, 29 (8), 1542–1546.
- (4) Zimmerman, M. L.; Daleke, D. L. Regulation of a Candidate Aminophospholipid-Transporting ATPase by Lipid1. *Biochemistry* **1993**, 32, 12257–12263.
- (5) Pomorski, T.; Muller, P.; Zimmermann, B.; Burger, K.; Devaux, P. F.; Herrmann, A. Transbilayer Movement of Fluorescent and Spin-Labeled Phospholipids in the Plasma Membrane of Human Fibroblasts: A Quantitative Approach. *J. Cell Sci.* **1996**, *109*, 687.
- (6) Pomorski, T.; Herrmann, A.; Müller, P.; Van Meer, G.; Burger, K. Protein-Mediated Inward Translocation of Phospholipids Occurs in Both the Apical and Basolateral Plasma Membrane Domains of Epithelial Cells †. *Biochemistry* 1999, 38, 142–150.
- (7) Paterson, J. K.; Renkema, K.; Burden, L.; Halleck, M. S.; Schlegel, R. A.; Williamson, P.; Daleke, D. L. Lipid Specific Activation of the Murine P 4-ATPase Atp8a1 (ATPase II). *Biochemistry* **2006**, 45, 5367–5376.
- (8) Papadopulos, A.; Vehring, S.; Lopez-Montero, I.; Kutschenko, L.; Stockl, M.; Devaux, P. F.; Kozlov, M.; Pomorski, T.; Herrmann, A. Flippase Activity Detected with Unlabeled Lipids by Shape Changes of Giant Unilamellar Vesicles. *J. Biol. Chem.* 2007, 282, 15559–15568.
- (9) Contreras, F. X.; Sánchez-Magraner, L.; Alonso, A.; Goñi, F. M. Transbilayer (Flip-Flop) Lipid Motion and Lipid Scrambling in Membranes. *FEBS Lett.* **2010**, *584* (9), 1779–1786.
- (10) Allhusen, J. S.; Conboy, J. C. The Ins and Outs of Lipid Flip-Flop. Acc. Chem. Res. 2017, 50 (1), 58-65.
- (11) Kornberg, R. D.; Mcconnell, H. M. Inside-Outside Transitions of Phospholipids in Vesicle Membranes. *Biochemistry* **1971**, *10* (7), 1111–1120.
- (12) Nakano, M.; Fukuda, M.; Kudo, T.; Matsuzaki, N.; Azuma, T.; Sekine, K.; Endo, H.; Handa, T. Flip-Flop of Phospholipids in Vesicles: Kinetic Analysis with Time-Resolved Small-Angle Neutron Scattering Flip-Flop of Phospholipids in Vesicles: Kinetic Analysis with Time-Resolved Small-Angle. *J. Phys. Chem. B* **2009**, *113*, 6745–6748.
- (13) Devaux, P. F.; Fellmann, P.; Hervé, P. Investigation on Lipid Asymmetry Using Lipid Probes: Comparison between Spin-Labeled Lipids and Fluorescent Lipids. *Chem. Phys. Lipids* **2002**, *116* (1–2), 115–134.
- (14) Marquardt, D.; Heberle, F. A.; Miti, T.; Eicher, B.; London, E.; Katsaras, J.; Pabst, G. 1H NMR Shows Slow Phospholipid Flip-Flop in Gel and Fluid Bilayers. *Langmuir* **2017**, *33* (15), 3731–3741.
- (15) Brzustowicz, M. R.; Brunger, A. T. X-Ray Scattering from Unilamellar Lipid Vesicles. *J. Appl. Crystallogr.* **2005**, *38*, 126–131.
- (16) Nakano, M.; Fukuda, M.; Kudo, T.; Matsuzaki, N.; Azuma, T.; Sekine, K.; Endo, H.; Handa, T. Flip-Flop of Phospholipids in Vesicles: Kinetic Analysis with Time-Resolved Small-Angle Neutron Scattering. *J. Phys. Chem. B* **2009**, *113*, 6745–6748.
- (17) Gerelli, Y.; Porcar, L.; Fragneto, G. Lipid Rearrangement in DSPC/DMPC Bilayers: A Neutron Reflectometry Study. *Langmuir* **2012**, 28 (45), 15922–15928.
- (18) McConnell, H. M.; Smith, B.; McConnell, H.; Langevin, D. Equilibration Rates in Lipid Monolayers. *Proc. Natl. Acad. Sci. U. S. A.* **1996**, 93 (26), 15001–15003.

- (19) Maekawa, M.; Fairn, G. D. Molecular Probes to Visualize the Location, Organization and Dynamics of Lipids. *J. Cell Sci.* **2014**, *127* (22), 4801–4812.
- (20) Gonzalez, M. A.; Barriga, H. M. G.; Richens, J. L.; Law, R. V.; O'Shea, P.; Bresme, F. How Does Ytterbium Chloride Interact with DMPC Bilayers? A Computational and Experimental Study. *Phys. Chem. Chem. Phys.* **2017**, *19* (13), 9199–9209.
- (21) Poznik, M.; Maitra, U.; König, B. The Interface Makes a Difference: Lanthanide Ion Coated Vesicles Hydrolyze Phosphodiesters. *Org. Biomol. Chem.* **2015**, *13* (38), 9789–9792.
- (22) Yamasaki, S.; Shirai, O.; Kano, K.; Kozai, N.; Sakamoto, F.; Ohnuki, T. Adsorption Behavior of Lanthanide Ions on Nonbiological Phospholipid Membranes: A Model Study Using Liposome. *Chem. Lett.* **2013**, 42, 819–821.
- (23) Nakano, M.; Fukuda, M.; Kudo, T.; Endo, H.; Handa, T. Determination of Interbilayer and Transbilayer Lipid Transfers by Time-Resolved Small-Angle Neutron Scattering. *Phys. Rev. Lett.* **2007**, 98, 238101.
- (24) Wah, B.; Breidigan, J. M.; Adams, J.; Horbal, P.; Garg, S.; Porcar, L.; Perez-Salas, U. Reconciling Differences between Lipid Transfer in Free-Standing and Solid Supported Membranes: A Time-Resolved Small-Angle Neutron Scattering Study. *Langmuir* **2017**, 33 (14), 3384–3394.
- (25) Heberle, F. A.; Marquardt, D.; Doktorova, M.; Geier, B.; Standaert, R. F.; Heftberger, P.; Kollmitzer, B.; Nickels, J. D.; Dick, R. A.; Feigenson, G. W.; Katsaras, J.; London, E.; Pabst, G. Subnanometer Structure of an Asymmetric Model Membrane: Interleaflet Coupling Influences Domain Properties. *Langmuir* **2016**, 32 (20), 5195–5200.
- (26) Doktorova, M.; Heberle, F. A.; Eicher, B.; Standaert, R. F.; Katsaras, J.; London, E.; Pabst, G.; Marquardt, D. Preparation of Asymmetric Phospholipid Vesicles for Use as Cell Membrane Models. *Nat. Protoc.* **2018**, *13* (9), 2086–2101.
- (27) Nguyen, M. H. L.; DiPasquale, M.; Rickeard, B. W.; Doktorova, M.; Heberle, F. A.; Scott, H. L.; Barrera, F. N.; Taylor, G.; Collier, C. P.; Stanley, C. B.; Katsaras, J.; Marquardt, D. Peptide-Induced Lipid Flip-Flop in Asymmetric Liposomes Measured by Small Angle Neutron Scattering. *Langmuir* 2019, 35 (36), 11735–11744.
- (28) Rickeard, B. W.; Nguyen, M. H. L.; Dipasquale, M.; Yip, C. G.; Baker, H.; Heberle, F. A.; Zuo, X.; Kelley, E. G.; Nagao, M.; Marquardt, D. Transverse Lipid Organization Dictates Bending Fluctuations in Model Plasma Membranes. *Nanoscale* **2020**, *12* (3), 1438–1447.
- (29) Joyce, R. E.; Williams, T. L.; Serpell, L. C.; Day, I. J. Monitoring Changes of Paramagnetically-Shifted31P Signals in Phospholipid Vesicles. *Chem. Phys. Lett.* **2016**, *648*, 124–129.
- (30) Prosser, R. S.; Hwang, J. S.; Vold, R. R. Magnetically Aligned Phospholipid Bilayers with Positive Ordering: A New Model Membrane System. *Biophys. J.* **1998**, *74*, 2405–2418.
- (31) Gonzalez, M. A.; Bresme, F. Membrane-Ion Interactions Modify the Lipid Flip-Flop Dynamics of Biological Membranes: A Molecular Dynamics Study. *J. Phys. Chem. B* **2020**, *124* (25), 5156–5162.
- (32) Liu, J.; Conboy, J. C. 1,2-Diacyl-Phosphatidylcholine Flip-Flop Measured Directly by Sum-Frequency Vibrational Spectroscopy. *Biophys. J.* **2005**, *89* (4), 2522–2532.
- (33) Anglin, T. C.; Conboy, J. C. Lateral Pressure Dependence of the Phospholipid Transmembrane Diffusion Rate in Planar-Supported Lipid Bilayers. *Biophys. J.* **2008**, *95* (1), 186–193.
- (34) Anglin, T. C., Cooper, M.; Li, H.; Chandler, K.; Conboy, J. C. Free Energy and Entropy of Activation for Phospholipid Flip-Flop in Planar Supported Lipid Bilayers. *J. Phys. Chem. B* **2010**, *114* (5), 1903–1914.
- (35) Anglin, T. C.; Conboy, J. C. Kinetics and Thermodynamics of Flip-Flop in Binary Phospholipid Membranes Measured by Sum-Frequency Vibrational Spectroscopy. *Biochemistry* **2009**, *48* (43), 10220–10234.
- (36) Liu, J.; Conboy, J. C. Phase Behavior of Planar Supported Lipid Membranes Composed of Cholesterol and 1,2-Distearoyl-Sn-Glycer-

- ol-3-Phosphocholine Examined by Sum-Frequency Vibrational Spectroscopy. Vib. Spectrosc. **2009**, 50 (1), 106–115.
- (37) Liu, J.; Conboy, J. C. Phase Transition of a Single Lipid Bilayer Measured by Sum-Frequency Vibrational Spectroscopy. *J. Am. Chem. Soc.* **2004**, *126* (29), 8894–8895.
- (38) Cicuta, P. Compression and Shear Surface Rheology in Spread Layers of β -Casein and β -Lactoglobulin. *J. Colloid Interface Sci.* **2007**, 308 (1), 93–99.
- (39) Liu, J.; Conboy, J. C. Structure of a Gel Phase Lipid Bilayer Prepared by the Langmuir-Blodgett/ Langmuir-Schaefer Method Characterized by Sum-Frequency Vibrational Spectroscopy. *Langmuir* **2005**, *21* (20), 9091–9097.
- (40) Liu, J.; Conboy, J. C. Structure of a Gel Phase Lipid Bilayer Prepared by the Langmuir-Blodgett/ Langmuir-Schaefer Method Characterized by Sum-Frequency Vibrational Spectroscopy. *Langmuir* **2005**, *21* (20), 9091–9097.
- (41) Marsh, D. Lateral Pressure in Membranes. *Biochim. Biophys. Acta. Biomembr.* 1996, 1286, 183–223.
- (42) Adams, E. M.; Casper, C. B.; Allen, H. C. Effect of Cation Enrichment on Dipalmitoylphosphatidylcholine (DPPC) Monolayers at the Air-Water Interface. *J. Colloid Interface Sci.* **2016**, 478, 353–364.
- (43) Firsching, F. H.; Brune, S. N. Solubility Products of the Trivalent Rare-Earth Phosphates. *J. Chem. Eng. Data* **1991**, *36* (1), 93–95.
- (44) Mullica, D. F.; Sappenfield, E. L.; Boatner, L. A. A Structural Investigation of Several Mixed Lanthanide Orthophosphates. *Inorg. Chim. Acta* 1990, 174 (2), 155–159.
- (45) Hong, H. Y.; Pierce, J. W. Crystal Structure of Ytterbium Ultraphosphate, YbP5O14. *Mater. Res. Bull.* **1974**, 9 (2), 179–189.
- (46) Demarco, P. V.; Elzey, T. K.; Lewis, R. B.; Wenkert, E. Paramagnetic Induced Shifts in the Proton Magnetic Resonance Spectra of Alcohols Using Tris(Dipivalomethanato)Europium(III). J. Am. Chem. Soc. 1970, 92 (19), 5734–5737.
- (47) Flockhart, B. D.; Jonas, J. Lanthanide Shift Reagents in Nuclear Magnetic Resonance Spectroscopy. *Crit. Rev. Anal. Chem.* **1976**, *6* (1), 69–130.
- (48) Rapuano, R.; Carmona-Ribeiro, A. M. Supported Bilayers on Silica. *J. Colloid Interface Sci.* **2000**, 226 (2), 299–307.
- (49) Pfefferlé, J.-M.; Bünzli, J. G. Interaction between the Buffer Tris and the Eu(III) Ion: Luminescence and Potentiometric Investigation. *Helv. Chim. Acta* **1989**, *72* (7), 1487–1494.
- (50) Oh, S. J.; Choi, Y.-S.; Hwangbo, S.; Bae, S. C.; Ku, J. K.; Park, J. W. Structure and Phosphodiesterase Activity of Bis-Tris Coordinated Lanthanide(III) Complexes. *Chem. Commun.* **1998**, *3*, 36–52.
- (51) Cicuta, P.; Terentjev, E. M. Viscoelasticity of a Protein Monolayer from Anisotropic Surface Pressure Measurements. *Eur. Phys. J. E* **2005**, *16* (2), 147–158.
- (52) Cicuta, P.; Stancik, E. J.; Fuller, G. G. Shearing or Compressing a Soft Glass in 2D: Time-Concentration Superposition. *Phys. Rev. Lett.* **2003**, *90* (23), 4.
- (53) Petkov, J. T.; Gurkov, T. D.; Campbell, B. E.; Borwankar, R. P. Dilatational and Shear Elasticity of Gel-like Protein Layers on Air/Water Interface. *Langmuir* **2000**, *16*, 3703–3711.
- (54) Espinosa, G.; Lopez-Montero, I.; Monroy, F.; Langevin, D. Shear Rheology of Lipid Monolayers and Insights on Membrane Fluidity. *Proc. Natl. Acad. Sci. U. S. A.* **2011**, *108* (15), 6008–6013.
- (55) You, S. S.; Rashkov, R.; Kanjanaboos, P.; Calderon, I.; Meron, M.; Jaeger, H. M.; Lin, B. Comparison of the Mechanical Properties of Self-Assembled Langmuir Monolayers of Nanoparticles and Phospholipids. *Langmuir* **2013**, *29* (37), 11751–11757.
- (56) Casillas-Ituarte, N. N.; Chen, X.; Castada, H.; Allen, H. C. Na+ and Ca2+ Effect on the Hydration and Orientation of the Phosphate Group of DPPC at Air-Water and Air-Hydrated Silica Interfaces Air-Water and Air-Hydrated Silica Interfaces. *J. Phys. Chem. B* **2010**, *114* (29), 9485–9495.
- (57) Spigone, E.; Cho, G. Y.; Fuller, G. G.; Cicuta, P. Surface Rheology of a Polymer Monolayer: Effects of Polymer Chain Length and Compression Rate. *Langmuir* **2009**, 25 (13), 7457–7464.

- (58) Allhusen, J. S.; Kimball, D. R.; Conboy, J. C. Structural Origins of Cholesterol Accelerated Lipid Flip-Flop Studied by Sum-Frequency Vibrational Spectroscopy. J. Phys. Chem. B 2016, 120, 3157-3168.
- (59) Mendelsohn, R.; Davies, M. A.; Brauner, J. W.; Schuster, H. F.; Dluhy, R. A. Quantitative Determination of Conformational Disorder in the Acyl Chains of Phospholipid Bilayers by Infrared Spectroscopy. Biochemistry 1989, 28 (22), 8934-8939.
- (60) Lehnert, R.; Eibl, H.-J.; Müller, K. Order and Dynamics in Lipid Bilayers from 1,2-Dipalmitoyl-Sn-Glycero-Phospho-Diglycerol as Studied by NMR Spectroscopy. J. Phys. Chem. B 2004, 108 (32), 12141-12150.
- (61) Anglin, T. C.; Liu, J.; Conboy, J. C. Facile Lipid Flip-Flop in a Phospholipid Bilayer Induced by Gramicidin A Measured by Sum-Frequency Vibrational Spectroscopy. Biophys. J. 2007, 92 (1), 3-5.
- (62) Nagle, J. F.; Tristram-Nagle, S. Structure of Lipid Bilayers. Biochem. Biophys. Acta 2000, 1469, 159-195.
- (63) John, K.; Schreiber, S.; Kubelt, J.; Herrmann, A.; Müller, P. Transbilayer Movement of Phospholipids at the Main Phase Transition of Lipid Membranes: Implications for Rapid Flip-Flop in Biological Membranes. Biophys. J. 2002, 83 (6), 3315-3323.
- (64) Brown, K. L.; Conboy, J. C. Phosphatidylglycerol Flip-Flop Suppression Due to Headgroup Charge Repulsion. J. Phys. Chem. B 2015, 119 (32), 10252-10260.
- (65) Hutton, W. C.; Yeagle, P. L.; Martin, R. B. The Interaction of Lanthanide and Calcium Salts with Phospholipid Bilayer Vesicles: The Validity of the Nuclear Magnetic Resonance Method for Determinatino of Vesicle Bilayer Phospholipid Surface Ratios. Chem. Phys. Lipids 1977, 19, 255-265.
- (66) Seelig, J.; Gaily, U. H.; Wohlgemuth, R.; Senko, E.; Templeton, H.; Shipman, J. J.; Folt, V. L.; Krimm, S.; Snyder, R. G.; Schachtschneider, J. H.; Sugeta, H.; Go, A.; Miyazawa, T.; Vieler, P.; Galsomias, J.; Yeagle, P. L.; Hutton, W. C.; Huang, C.; Martin, R. B. Interaction of Metal Ions with Phosphatidylcholine Bilayer Membranes. Spectrochim. Acta, Part A 1981, 20, 4344-4348.
- (67) Haverstick, D. M.; Glaser, M. Visualization of Domain Formation in the Inner and Outer Leaflets of a Phospholipid Bilayer. J. Cell Biol. 1988, 106, 1885-1892.
- (68) Brown, K. L.; Conboy, J. C. Lipid Flip-Flop in Binary Membranes Composed of Phosphatidylserine and Phosphatidylcholine. J. Phys. Chem. B 2013, 117 (48), 15041-15050.

□ Recommended by ACS

Understanding the Molecular Mechanism of Anesthesia: Effect of General Anesthetics and Structurally Similar Non-**Anesthetics on the Properties of Lipid Membranes**

Zsófia B. Rózsa, Pál Jedlovszky, et al.

JUNE 27, 2023

THE JOURNAL OF PHYSICAL CHEMISTRY B

RFAD 🗹

Charged Lipids Modulate the Phase Separation in Multicomponent Membranes

Yifei Wang and Sheereen Majd

JULY 24, 2023

LANGMUIR

READ 1

Depth-Dependent Segmental Melting of the Sphingomyelin Alkyl Chain in Lipid Bilayers

Hiroshi Tsuchikawa, Michio Murata, et al.

APRIL 28, 2022

LANGMUIR

READ C

Orientation of Cholesterol in Polyunsaturated Lipid Bilayers

Iain M. Braithwaite and James H. Davis

DECEMBER 08, 2022

LANGMUIR

READ C

Get More Suggestions >